Materials Research Bulletin 62 (2015) 153–160

Contents lists available at ScienceDirect

Materials Research Bulletin

journal homepage: www.elsevier.com/locate/matresbu

Structural and transport properties of double perovskite Dy_2NiMnO_6

Sadhan Chanda *, Sujoy Saha, Alo Dutta, T.P. Sinha

Department of Physics, Bose Institute, 93/1, Acharya Prafulla Chandra Road, Kolkata 700009, India

ARTICLE INFO

Article history:
Received 10 June 2014
Accepted 8 November 2014
Available online 11 November 2014

Keywords:
A. Ceramics
B. Sol–gel chemistry
C. Impedance spectroscopy
D. Dielectric properties
E. Electronic structure

ABSTRACT

The double perovskite oxide Dy_2NiMnO_6 (DNMO) is synthesized in nano and bulk phase by the sol–gel citrate method. The Rietveld refinement of X-ray diffraction pattern of the sample at room temperature shows the monoclinic $P2_1/n$ phase. Dielectric relaxation of the sample is investigated in the impedance and electric modulus formalisms in the frequency range from 50 Hz to 1 MHz and in the temperature range from 253 to 415 K. The Cole–Cole model is used to explain the relaxation mechanism in DNMO. The frequency-dependent maxima in the imaginary part of impedance are found to obey an Arrhenius law with activation energy of 0.346 and 0.344 eV for nano and bulk DNMO, respectively. A significant increase in conductivity of bulk DNMO has been observed than that of the nanoceramic. Electronic structures and magnetic properties of DNMO have been studied by performing first principles calculation based on density functional theory.

1. Introduction

Multifunctional double perovskite oxides (DPOs) Ln_2NiMnO_6 [Ln = lanthanides] have gained immense research interest in the recent years due to their rich physical properties which make them as the prospective materials for technological applications [1–13]. In this family La_2NiMnO_6 having ferromagnetic order temperature of about 280 K is a rare example of a single material platform with multiple functions, in which the spins, electric charges, and dielectric properties can be tuned by magnetic and/or electric fields. The dielectric relaxor behaviour is also observed in Nd_2NiMnO_6 by Shi et. al [4]. These properties make this series of materials suitable for possible applications in spintronic devices, such as magnetic memories and magnetodielectric capacitors [2,6].

Most of the reported Ln_2NiMnO_6 DPOs have been prepared by high temperature solid-state reaction technique from their corresponding pure oxides. But in many cases this technique suffers from the problem of the presence of some unreacted rare earth oxides as impurities in the materials and sometimes the formation of undesirable phases [7]. It is observed that probability of getting the impurity phases increases when the ionic radius of the rare earth element in this series decreases [11,12]. In this respect while synthesising Tb_2NiMnO_6 by solid state reaction technique, the existence of an impurity phase of Tb_2O_3 is reported by Nair et al. [11]. Similarly, Y_2NiMnO_6 [12] has not been synthesised in single phase because radius of Y^{3+} is almost equal to Dy^{3+}. Thus, synthesizing a pure phase material of this family with lower ionic radius (such as Y, Dy–Lu compounds) is challenging.

Among the various Ln_2NiMnO_6 DPOs studied so far, Dy_2NiMnO_6 (DNMO) is a ferromagnetic material with $T_c \sim 105$ K. Asai et al. have studied the crystal structure and magnetic properties of DNMO and concluded that superexchange interaction Ni^{2+}–O–Mn^{4+} is responsible for ferromagnetism in this material [7]. The theoretical effort for understanding the various microscopic properties of DNMO is not available in the literature. To our knowledge, there exists no report of plane wave based basic electronic structure calculation of DNMO.

In the present work, we have successfully synthesised a pure phase of DNMO by sol–gel citrate method. The dielectric properties of the sample have been investigated by alternating current impedance spectroscopy (ACIS) in a frequency range from 50 Hz to 1 MHz and in the temperature range from 253 K to 415 K. The study of the influence of sintering conditions (effects of grain size) on the electrical properties of the ceramic has also been reported. We have carried out the spin polarised density functional theory calculations using full potential linearized augmented plane wave (FPLAPW) method implemented in WIEN2k [14] to understand the ferromagnetic insulating behaviour in this compound.

2. Experimental

2.1. Sample preparation

DNMO in powder form was synthesized by the sol–gel citrate method [15,16]. At first, reagent grade $Dy(NO_3)_3 \cdot 6H_2O$ (Alfa Aesar),

* Corresponding author. Tel.: +91 33 23031191/9836626460; fax: +91 33 23506790.
E-mail addresses: sadhan.physics@gmail.com, schanda.cob@gmail.com (S. Chanda).

http://dx.doi.org/10.1016/j.materresbull.2014.11.021
0025-5408/

$Ni(NO_3)_2{\cdot}4H_2O$ (Alfa Aesar), and $Mn(NO_3)_2{\cdot}6H_2O$ (Alfa Aesar) were taken in stoichiometry ratio and separately dissolved in de-ionized water by stirring with a magnetic stirrer. The obtained clear solutions were then mixed together. Citric acid (CA) and ethylene glycol (EG) were added to this solution drop wise according to the molar ratio of $\{Dy^{3+}, Ni^{2+}+Mn^{2+}\}$:{CA}:{EG} = 1:1:4 to form a polymeric-metal cation network. The solution was stirred at 348 K using a magnetic stirrer for 4 h to get a homogeneous mixture and then the solution was dried at 393 K to obtain the gel precursor. At the end, combustion had taken place in the gel which had produced a black fluffy powder of the material. The powder was calcined at 1073 K in air for 5 h and cooled down to room temperature (RT ~ 300 K) at a cooling rate of 1 K/min. The calcined sample was pelletized into discs of thickness = 1.5 mm and diameter = 8 mm using polyvinyl alcohol as binder. Finally, these pellets were sintered at 1073 and 1423 K for 10 h in air and cooled down to RT by cooling at the rate of 1 K/min. From now onwards, we have abbreviated DNMO-1 and DNMO-2 for the samples sintered at 1073 and 1423 K, respectively.

2.2. Sample characterization

The determination of lattice parameters and the identification of the phase at RT was carried out using a X-ray powder diffractometer (Rigaku Miniflex II) having Cu-Kα radiation in the 2θ range of 15–80° by scanning at 0.02° per step. The refinement of crystal structure was performed by the Rietveld method with the Fullprof program [17]. The background was fitted with 6-coefficients polynomial function, while the peak shapes were described by pseudo-Voigt profiles. Throughout the refinement, scale factor, lattice parameters, positional coordinates (x, y, z), and thermal parameters were varied and the occupancy parameters of all the ions were kept fixed. The particle size and selected area electron diffraction (SAED) pattern of the sample (DNMO-1) were studied by the high resolution transmission electron microscopy (HRTEM) (FEI Tecnai G2, 200 KV). The scanning electron microscope (FEI Quanta 200) was used for investigation of the homogeneity of the synthesized samples. The optical spectrum of the material was collected by a Shimadzu UV–vis spectrometer.

For electrical measurements, both the sides of sintered pellets were polished. Two thin gold plates were used as electrodes. The impedance, conductance, and phase angle were measured using an LCR meter (HIOKI) in the frequency range from 50 Hz to 1 MHz at the oscillation voltage of 1.0 V. The measurements were performed over the temperature range from 253 K to 415 K using an inbuilt cooling–heating system. The temperature was controlled by an Eurotherm 2216e programmable temperature controller connected with the oven. Each measured temperature was kept constant with an accuracy of ±1 K. The complex dielectric modulus M^* ($=j\omega C_o Z^*$) was obtained from the temperature dependence of the real (Z') and imaginary (Z'') components of the complex impedance Z^* ($=Z'+iZ''$), where ω is the angular frequency ($\omega = 2\pi\nu$) and $i=\sqrt{-1}$. $C_o = \varepsilon_o A/d$ is the empty cell capacitance, where A is the sample area, and d is the sample thickness. The I–V characteristics of DNMO were measured in the temperature range from 213 K to 473 K using a source measure unit (Keithley 236).

2.3. Computational details

The experimental lattice parameters are used as the input for the FPLAPW calculations of DNMO. The muffin-tin (MT) radii for Dy, Ni, Mn, and O are taken as 2.21, 1.96, 1.91, and 1.65 au (atomic unit), respectively. To take into account the exchange and correlation effects, generalized gradient approximation (GGA) as parametrized by Perdew et al. [18] has been applied. No shape approximation corresponding to potential is taken into account. In the calculations, we have used a parameter $R_{MT}K_{max} = 7$, which determines matrix size (convergence), where K_{max} is the plane wave cut-off and R_{MT} is the smallest of all atomic sphere radii. For the self-consistent calculation with the plane wave basis $4\times4\times4$ Monkhorst-Pack [19] k point mesh is used. The iteration process is continued until calculated total energy and charge density of the crystal converged and becomes less than 0.01 mRy/unit cell and 0.001 e/a.u.^{3}, respectively. For the 3d transition metal (Ni and Mn) and rare earth element (Dy) the correlation effect of localized d and f electrons are considered. We have applied the effective Coulomb potential ($U_{Ni-3d} = U_{Mn-3d} = 2$ eV and $U_{Dy-4f} = 4$ eV) in GGA + U [20] calculations. The value of U is optimized such that the moments of the magnetic ions and optical band gap are satisfactorily described with respect to the experimental results.

3. Results and discussion

3.1. Structural analysis

The X-ray diffraction pattern of DNMO-1 is shown in Fig. 1, where the symbols represent the experimental data and the solid line represents the best fit to the diffraction data obtained by Rietveld refinement for monoclinic symmetry (space group $P2_1/n$). The curve at the bottom represents the difference between experimental pattern and the calculated one. The refined lattice parameters, $a = 5.2425(4)$ Å, $b = 5.5468(5)$ Å, $c = 7.5025(7)$ Å, and the monoclinic angle $\beta = 90.042(2)°$ are in reasonable agreement with the same series of materials such as Tb_2NiMnO_6 [11] and Ln_2NiMnO_6 (Ln=Nd, Sm) [9]. The stability of DNMO to a first approximation is determined by the ratio of Dy—O to B—O (B=Ni, Mn) bond lengths, which can be expressed as the tolerance factor $T_f = (r_{Dy}+r_0)/(\sqrt{2}((r_{Ni}+r_{Mn})/2+r_0))$ (where r_{Dy}, r_{Ni}, r_{Mn}, and r_o are ionic radii of dysprosium, nickel, manganese, and oxygen, respectively). Here Dy has co-ordination number eight instead of 12. The reduced coordination number of Dy is a result of some of the anions moving too far away for lower symmetry DPO due to octahedral tilting which causes the first coordination sphere about the Dy cation to change. It has been proposed by Woodward [21] that any anion more than 3.00 Å away from the A-cation of DPOs (general formula $A_2B'B''O_6$) may be considered to be outside the coordination sphere. It is found that $T_f = 0.85$ for DNMO using $r_{Dy} = 1.027$ Å, $r_{Ni} = 0.69$ Å, $r_{Mn} = 0.53$ Å, and $r_o = 1.4$ Å [22]. A schematic presentation of the DNMO cell is shown in the inset of Fig. 1 with the distribution of ions at crystallographic positions 4e for

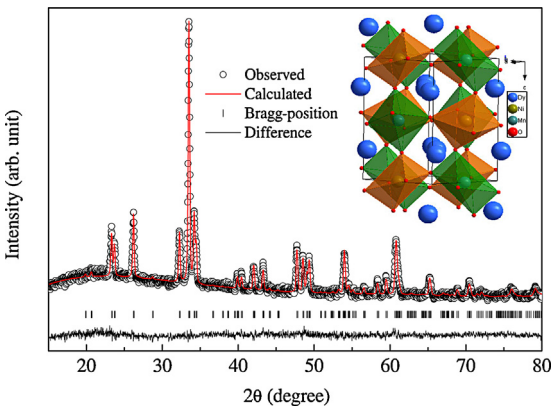

Fig. 1. Rietveld refinement plot of DNMO-1 at room temperature. A schematic presentation of the DNMO monoclinic unit cell is shown in the inset. The Ni atoms are located at the centres of the NiO_6 (orange) octahedra. The Mn atoms are located at the centres of the MnO_6 (green) octahedral. (For interpretation of the references to color in this figure legend, the reader is referred to the web version of this article.)